Geophysical Research Letters

RESEARCH LETTER
10.1029/2019GL086841

COSMIC-2 Radio Occultation Constellation: First Results

W.S. Schreiner[1], J.P. Weiss[1], R.A. Anthes[1], J. Braun[1], V. Chu[2], J. Fong[2], D. Hunt[1], Y.-H. Kuo[1], T. Meehan[3], W. Serafino[4], J. Sjoberg[1], S. Sokolovskiy[1], E. Talaat[4], T.K. Wee[1], and Z. Zeng[1]

[1]COSMIC Program, University Corporation for Atmospheric Research, Boulder, CO, USA, [2]National Space Organization, Hsinchu, Taiwan, [3]Jet Propulsion Laboratory, NASA, Pasadena, CA, USA, [4]NESDIS, NOAA, Silver Spring, MD, USA

Key Points:
- First operational tropical constellation of radio occultation (RO) satellites is collecting atmospheric bending angles and refractivity profiles of unprecedented quality
- Six advanced Global Navigation Satellite System (GNSS) RO receivers provide up to 5,000 high signal-to-noise ratio (SNR) profiles per day in the tropics
- First publicly available RO data from GLONASS (GLObal Navigation Satellite System)

Correspondence to:
R.A. Anthes,
anthes@ucar.edu

Citation:
Schreiner, W. S., Weiss, J. P., Anthes, R. A., Braun, J., Chu, V., Fong, J., et al. (2020). COSMIC-2 radio occultation constellation: First results. *Geophysical Research Letters*, *47*, e2019GL086841. https://doi.org/10.1029/2019GL086841

Received 26 DEC 2019
Accepted 31 JAN 2020
Accepted article online 05 FEB 2020

Abstract Initial data from the Formosa Satellite-7/Constellation Observing System for Meteorology Ionosphere and Climate (FORMOSAT-7/COSMIC-2, hereafter C2), a recently launched equatorial constellation of six satellites carrying advanced radio occultation receivers, exhibit high signal-to-noise ratio, precision, and accuracy, and the ability to provide high vertical resolution profiles of bending angles and refractivity, which contain information on temperature and water vapor in the challenging tropical atmosphere. After an initial calibration/validation phase, over 100,000 soundings of bending angles and refractivity that passed quality control in October 2019 are compared with independent data, including radiosondes, model forecasts, and analyses. The comparisons show that C2 data meet expectations of high accuracy, precision, and capability to detect superrefraction. When fully operational, the C2 satellites are expected to produce ~5,000 soundings per day, providing freely available observations that will enable improved forecasts of weather, including tropical cyclones, and weather, space weather, and climate research.

Plain Language Summary This paper describes an initial quality assessment of satellite observations from a recently launched (25 June 2019) constellation of six satellites that orbit Earth over the tropics. The approximately 5,000 vertical profiles per day, obtained using a relatively new technique called radio occultation, provide information of unprecedented quality on the temperature and water vapor in the tropics. These observations, which are freely available to forecasters and researchers worldwide, will be useful in improving forecasts of weather, including tropical cyclones, and supporting weather and climate research.

1. Introduction

COSMIC-2 (C2), a Taiwan-United States six-satellite mission, was launched on 25 June 2019 (Anthes & Schreiner, 2019). Each satellite carries an advanced Tri-GNSS (Global Navigation Satellite System) Radio Occultation (RO) System instrument (TGRS) developed by National Aeronautics and Space Administration's Jet Propulsion Laboratory (Tien et al., 2012). The TGRS includes a high-gain beam-forming RO antenna, and is achieving the highest signal-to-noise ratio (SNR) of RO measurements to date (>2,500 V/V in a 1 Hz band). When fully operational, the C2 satellites are expected to produce 5,000 high vertical resolution profiles of bending angles and refractivity per day in the tropics and subtropics. The bending angles and refractivity can be directly assimilated in numerical weather prediction models. They may also be used with ancillary data to derive accurate vertical profiles of temperature and water vapor (Li et al., 2019), but this process and these derived variables are beyond the scope of this article. C2 will also provide data arcs of total electron content (TEC) and vertical profiles of electron density in the ionosphere to support space weather operations and research. C2 is an operational follow-on to the FORMOSAT-3/COSMIC (hereafter COSMIC) research mission launched in 2006 (Anthes, 2011; Ho et al., 2019) and is a successful example of a research-to-operations transition. This paper takes a first look at the quality of the C2 RO data by comparing them with other independent data sets, including operational radiosondes, short-term operational model forecasts, and MERRA-2 reanalyses (Gelaro et al., 2017). Most of the comparisons use over 100,000 C2 profiles from October 2019, after an initial calibration/validation phase.

By May 2021 the C2 satellites will be deployed into six evenly spaced circular orbital planes of 24° inclination at an altitude of about 550 km. In addition to the TGRS, each satellite carries two space weather instruments, the Ion Velocity Meter (IVM, Heelis et al., 2017) and the Radio Frequency Beacon (RFB). The IVM measures

in situ ion temperature, velocity, and density. The RFB is a transmitter that enables measurements of TEC and ionospheric scintillation by ground receivers. These instruments will contribute to the forecasting of space weather events, monitoring and prediction of scintillation (e.g., Equatorial plasma bubbles and sporadic E-clouds), and understanding of the coupling between the lower and upper atmosphere. Results from these instruments will be presented in the future.

A network of 10 downlink ground stations, located in Australia, Brazil, French Polynesia, Ghana, Guam, Hawaii, Honduras, Kuwait, Mauritius, and Taiwan, receives data and routes them to Taiwan and the United States for processing. This network enables C2 data to be made available in near-real time (more than half the observations processed within 30 min) for use in numerical weather prediction (NWP) and space weather prediction. The data are freely available and may be obtained from the COSMIC Data Analysis and Archive Center (CDAAC, www.cosmic.ucar.edu). Information about and how to download the data are presented in the document *FORMOSAT-7/COSMIC-2 Neutral Atmospheric Provisional Release 1* available on the CDAAC web site.

2. Initial Results

2.1. SNR and Other Characteristics of C2 RO Soundings

C2 is producing higher SNR values than any previous RO mission, owing to the advanced TGRS receiver and high-gain antenna. Early results indicate that the mean SNR in the 60–80 km height range of the GPS (Global Positioning System) L1 signal is over 1,500 V/V, with significant numbers of occultations measuring L1 SNRs exceeding 2,000 V/V (Figure 1a). This is much higher than the average SNR of COSMIC of ~800 V/V. Higher SNR reduces the contribution of thermal noise to bending angle (BA) errors. BA observational errors are commonly characterized by the standard deviation (SD) of retrieved BA from climatology between 60 and 80 km, where the main error contributors are thermal noise, ionospheric residuals, and GNSS clock errors.

High SNR is important in at least three ways: penetration of soundings lower into the troposphere, detection of sharp atmospheric boundary layer (ABL) tops, and detection of super-refraction (SR) on top of the ABL. Figure 2a shows penetration depths above ground level for C2 and eight other RO missions for occultations colocated with C2 soundings within 200 km and 2 hr. Penetration depth depends on many factors, for example, data processing, geographic region, season, and may be different for rising and setting occultations. Also, the difference between results from different processing centers may depend on the RO instrument (Syndergaard, 2018). Standard CDAAC processing was applied for all RO missions to make the penetration depths as comparable as possible. The factors mentioned above do not affect the main result of Figure 2a, which shows that C2 provides deeper penetration of profiles compared to other RO missions, with 50% reaching within 200 m of the surface.

Figure 2b shows the penetration depth above mean sea level (MSL) for C2 occultations over the oceans, as function of L1 SNR for GPS and GLONASS, and indicates that higher SNR allows deeper penetration.

Sharp ABL tops can be detected at the heights of maximum BA lapse (BAL, Sokolovskiy et al., 2007). Examples of large BAL can be seen in Figures 3g–3i around 1.5–2 km heights. Figure 2c shows BAL > 0.01 rad, globally, as a function of L1 SNR. Higher SNR allows retrievals of BA profiles with larger BAL, thus increasing the reliability of detection of sharp ABL tops. In order to rule out the effect of possible geographical variations of the SNR, we also calculate BAL versus SNR for two separate regions known for sharp ABL tops: west of Africa (15°W to 10°E, 40–0°S) and west of South America (105–80°W, 40–0°S), also shown in Figure 2c. Though BAL is larger in those regions (to be expected), its dependence on SNR is about the same as with the global data.

SR on top of the ABL is a known problem for RO data assimilation (e.g., Xie et al., 2010). NWP models can reproduce SR, but their predictions may contain errors and so direct observations of SR are useful for NWP as well as weather and climate research. SR can be detected by the existence of deep signals in spectrograms of RO signals acquired under high SNR (Sokolovskiy et al., 2014). Figure 3 shows three C2 occultations tracked down to −350 km height of the tangent point (TP) of the straight line from the transmitter to receiver. Panels (a)–(c) show SNRs. Panels (d)–(f) show spectrograms of RO signals down-converted using a model based on orbit geometry and refractivity climatology (to reduce frequency). Panels (g)–(i) show BA

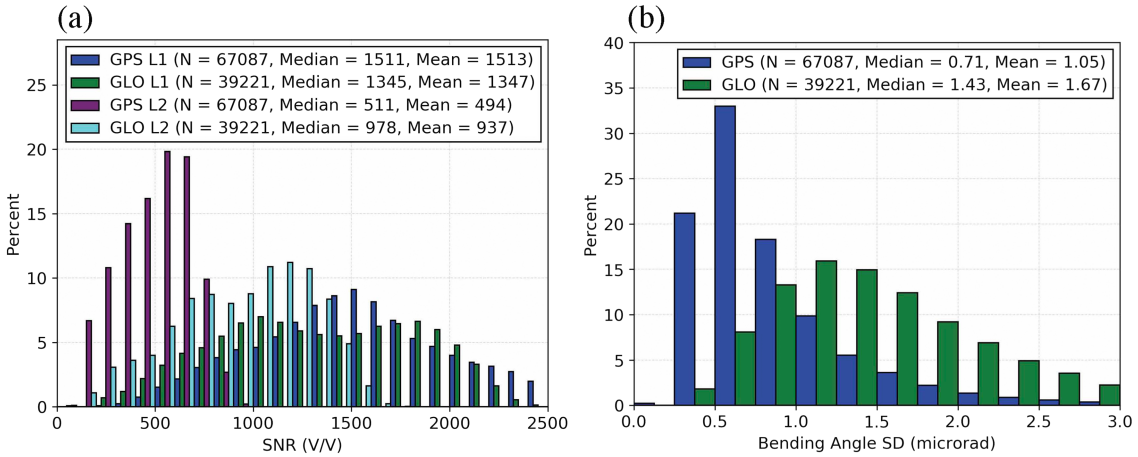

Figure 1. (a) Histograms of SNR for GPS L1 (dark blue) and L2 (L2P and L2C, purple) and GLONASS L1 (green) and L2 (light blue) signals. (b) Histograms of SD of BA for GPS (blue) and GLONASS (green) occultations. Larger SD for GLONASS is related to larger transmitter clock interpolation errors, which may be reduced by reducing interpolation intervals (currently 30 s for near-real-time processing).

profiles obtained from C2 and forward modeled (Gilpin et al., 2019) from European Centre for Medium Range Weather Forecasts (ECMWF) short-range forecasts interpolated to the time, latitude, and longitude of the "occultation point" (Kuo et al., 2004). All BA profiles indicate sharp tops of the ABL (large BAL). The ECMWF profiles stop at the height of SR because the BA equals infinity at this point. Spectrogram (d) does not show any signal below −150 km, thus no SR, while (e) and (f) show deep signals well below −150 km, thus detecting SR. ECMWF agrees with RO in cases (g) and (h), but not in case (i) where it does not show the SR detected from the RO spectrogram (f).

2.2. Precision Estimates From Intracomparison of C2 Satellite Data

Following the launch, the C2 satellites were located close together for a short period of time, enabling estimation of the precision of the BA retrievals by comparing the BA from two nearby satellites at nearly the same time with similar occultation geometry. Figure 4 shows the mean and SD of the differences of 265 pairs of quality-controlled C2 soundings (GPS and GLONASS) with horizontal separations of TP < 20 km from 16

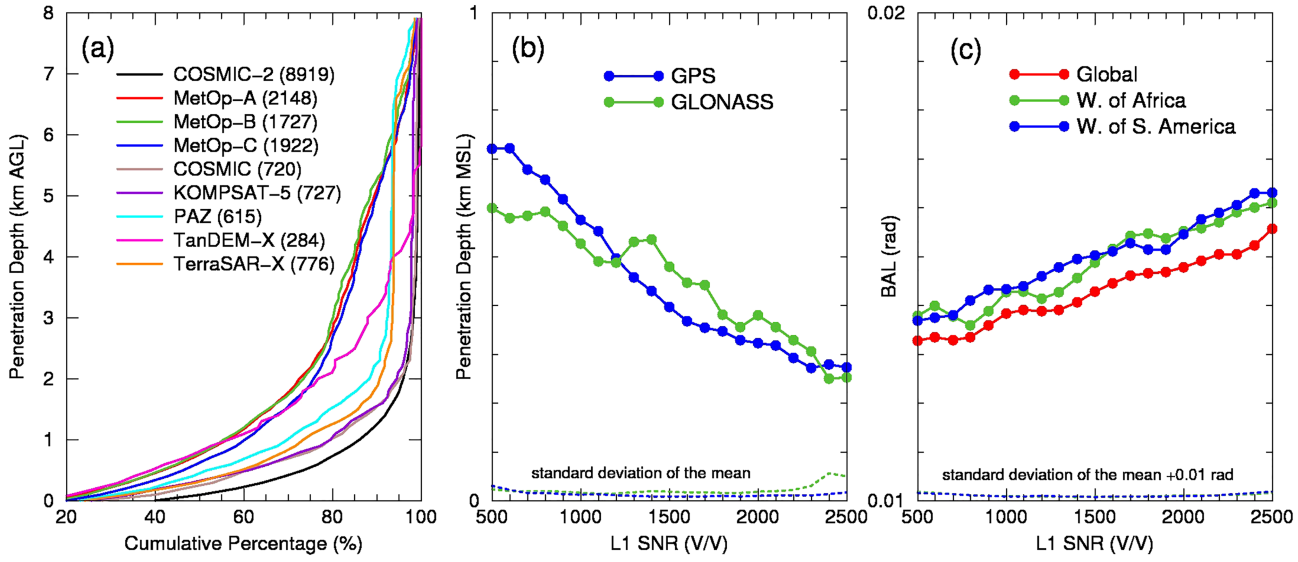

Figure 2. (a) Distributions of the penetration depths (minimum heights above ground level of colocated profiles) for C2 (black profile) and eight other RO missions. The number of soundings for each mission is shown in parentheses in the mission label. (b) C2 penetration depths as functions of L1 SNR for GPS and GLONASS. (c) BAL as function of L1 SNR globally and in two local regions. Panels (b) and (c) represent averaged values in ±100 V/V bin.

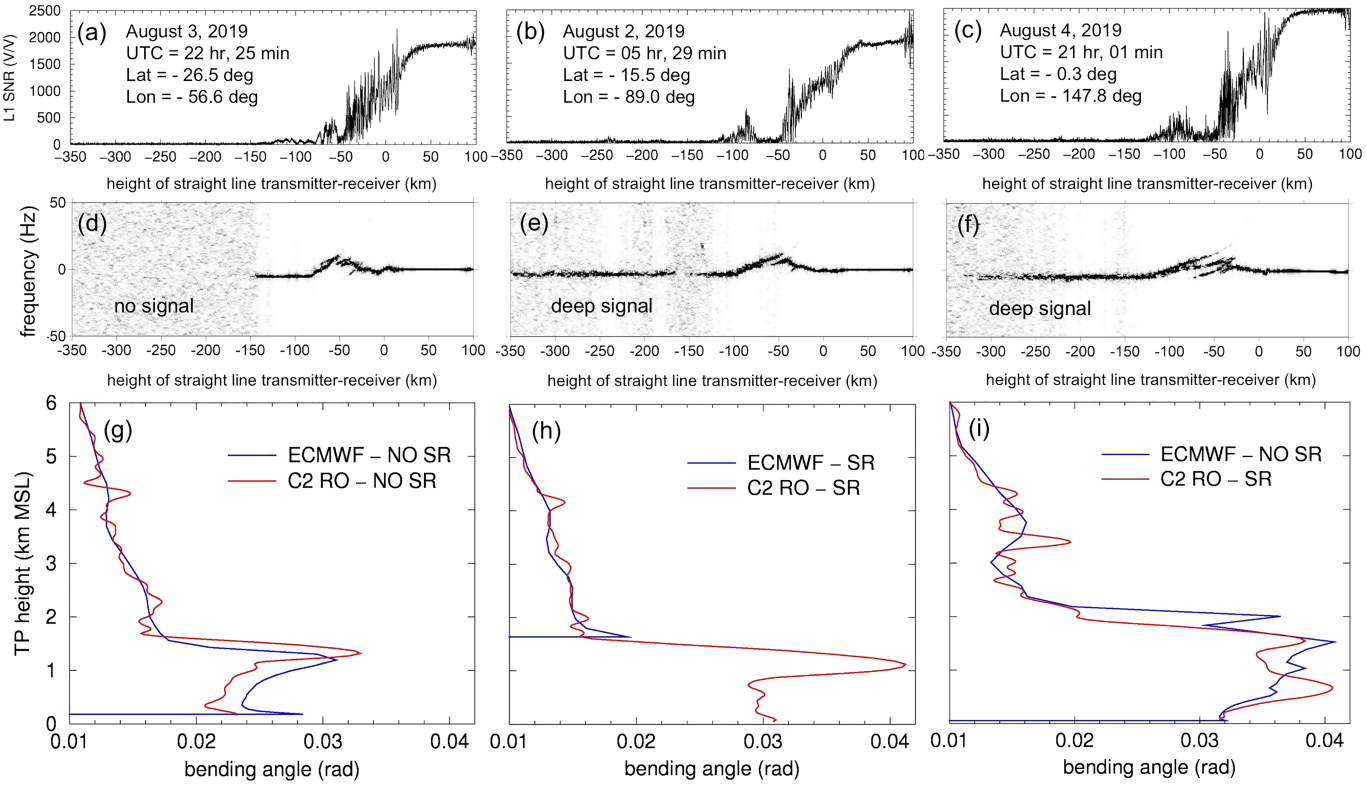

Figure 3. (a)–(c) SNR for three C2 occultations. (d) –(f) Spectrograms of RO signals down-converted using frequency model (see text). (g)–(i) BA as function of ray TP height above MSL for C2 RO (red) and ECMWF (blue).

July to 4 September 2019 between 10 and 60 km altitude. There is a very small bias and a SD of approximately 2.2 microradians between 30 and 60 km and less than about 30.0 microradians between 10 and 30 km. Under the assumption that paired soundings have uncorrelated errors of the same magnitudes, the random

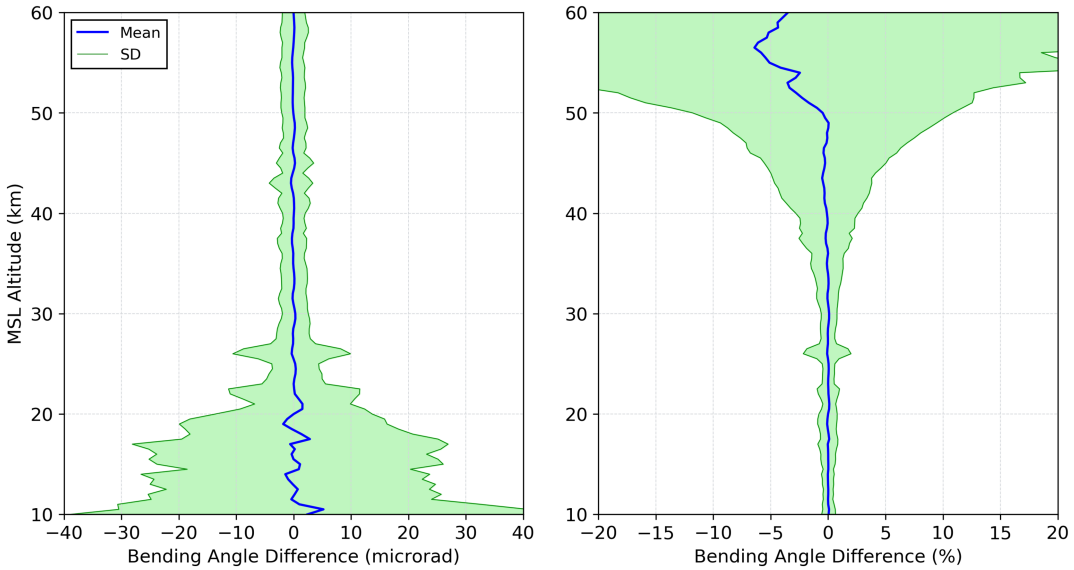

Figure 4. Mean and SD of BA differences from 265 pairs of nearby C2 satellites between 10 and 60 km. (a) Absolute differences; (b) percentage differences. Several outliers (due to the norming of the differences with noisy observables that occasionally are close to zero at high altitudes) are removed for display purposes from panel (b) only. The MSL altitude is the altitude of the ray TP.

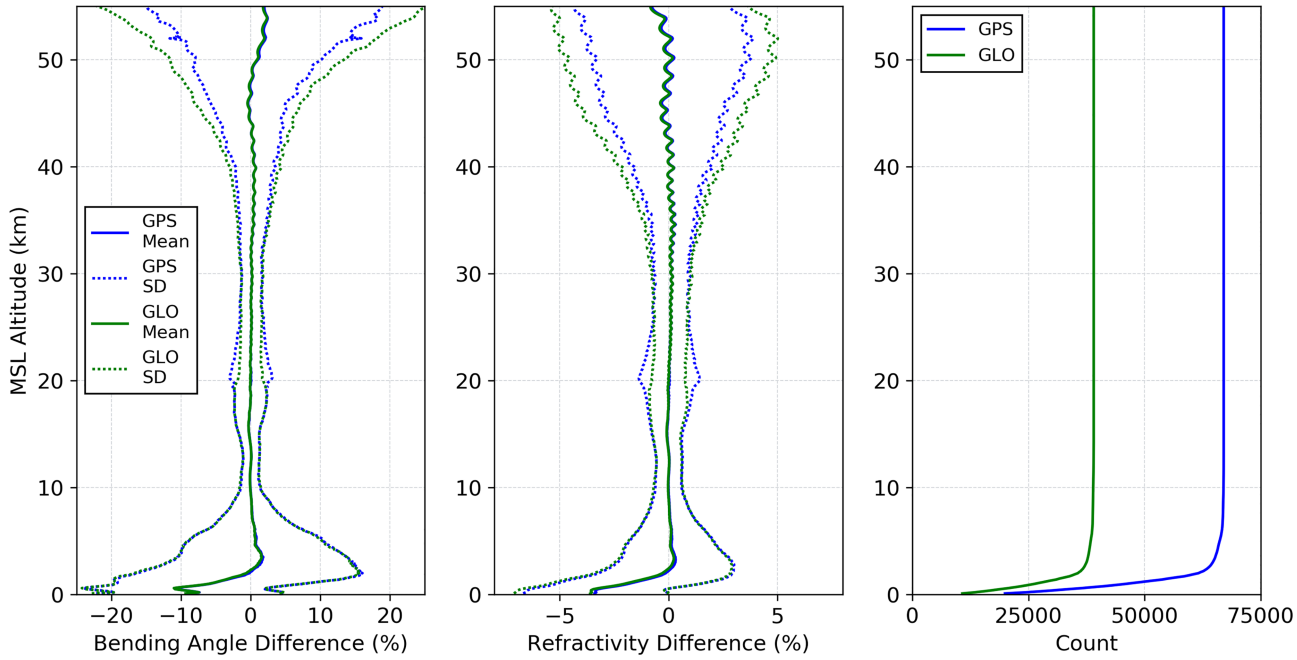

Figure 5. (left) Mean and SD of differences in BA between C2 and ECMWF from GPS (blue) and GLONASS (green) occultations. (middle) Same as left panel except for refractivity. (right) Counts of GPS (blue) and GLONASS (green) occultations. The MSL altitude is the altitude of the ray TP. The percentage differences are <(C2-ECMWF)/ECMWF> where < > is the sample mean. Wavy structures above 30 km are related to linear interpolation on the ECMWF model grid.

uncertainty of individual sounding (the precision) is estimated to be the SD divided by the square root of 2. This results in a precision estimate of ~1.6 microradians for the 30–60 km altitude range, which is well below the C2 mission requirement value of 2.0 microradians.

2.3. Comparison With Other Data Sets

We compared the October 2019 C2 data set with operational radiosondes (RS), short-term forecasts from the National Centers for Environmental Prediction (NCEP) and ECMWF forecast models, and the MERRA-2 reanalysis. Figure 5 shows the mean and SD of the differences between the BA and refractivity profiles from C2 and colocated ECMWF operational short-term forecasts. Both the GPS and GLONASS retrievals are consistent with each other and show very small biases compared to ECMWF between 6 and 40 km, some minor positive biases between 2 and 6 km, and negative biases below 2 km. RO biases in the lower troposphere are known to be caused by a combination of different factors: SR (affects refractivity; Ao et al., 2003; Ao, 2007; Sokolovskiy, 2003; Xie et al., 2006; Xie et al., 2010), tracking depth and noise (Sokolovskiy, 2003; Sokolovskiy et al., 2010), and fluctuations of refractivity (Gorbunov et al., 2015; Gorbunov & Kirchengast, 2018). Analysis of RO biases, their dependence on the processing and the SNR and their reduction in the C2 processing is complicated and is the subject of a separate study. The increased SD at ~19–25 km for GPS is thought to be due to a technical problem when tracking L2P signals that is expected to be resolved in the future.

The three-cornered hat (3CH) method (Anthes & Rieckh, 2018, hereafter AR2018; Rieckh & Anthes, 2018) is used to estimate the random error SD (uncertainty) of the C2 refractivity observations using four other data sets (listed in the caption of Figure 6). The model data sets are interpolated to the locations, times, and mandatory levels of the operational radiosondes (RS), while RO data within 3 hr and 300 km of the RS locations are interpolated in the vertical to the RS mandatory levels. The 3CH equations include bias correction terms, which remove biases among the data sets (O'Carroll et al., 2008). The major limitation of the 3CH method, the potential correlation of errors between the four data sets and C2, is expected to be small since the October 2019 C2 data were not assimilated in any of the models or reanalyses.

Figure 6 shows the 3CH results for the five data sets. Five data sets produce six independent 3CH estimates of the error SD. The small SD of differences of the six estimates (shading about the mean) indicates the effect of any correlations of errors is small. For these data sets the ECMWF and NCEP Global Forecast System

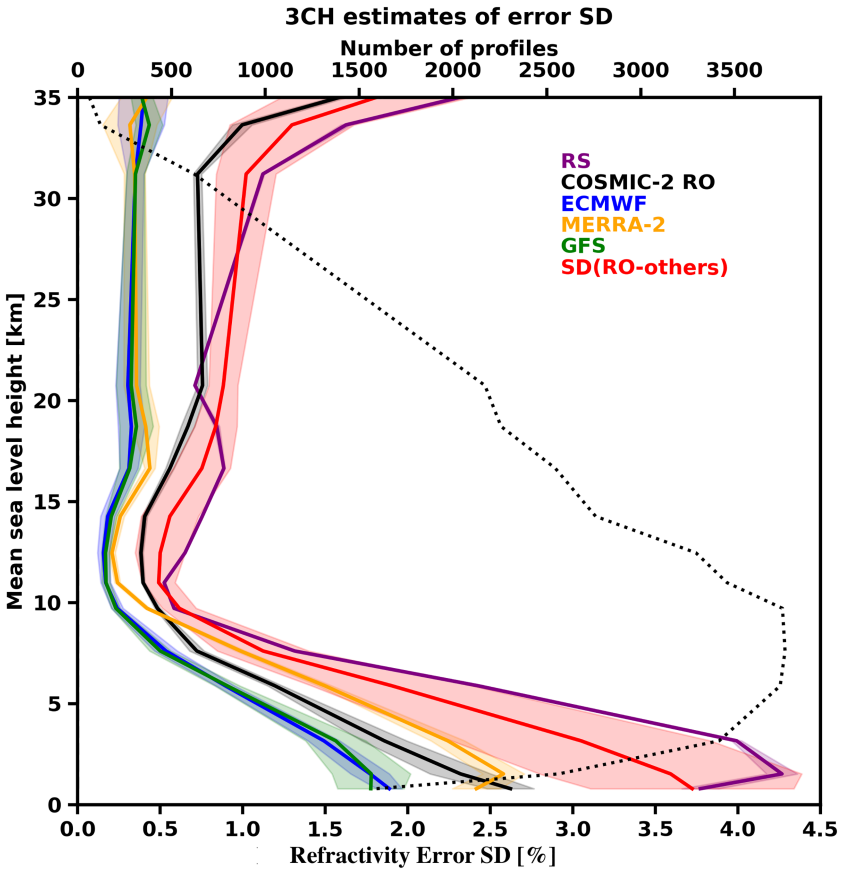

Figure 6. 3CH estimates of refractivity error SD of COSMIC-2 (black), ECMWF analysis (blue), NCEP GFS analysis (green), MERRA-2 reanalysis (orange), and radiosondes (purple). The mean of the six SD estimates for each data set are the solid lines and the SD around this mean is indicated by the shading. Also shown is the mean SD of differences between C2 and each of the other four data sets (red) and the SD around this mean (red shading). The number of colocated data points (sample size) is shown by the dotted line. Profiles below 925 hPa (about 750 m) are not shown because of small sample size and potential lower boundary effects on the colocation procedure.

analyses show the smallest SD of errors, while the RS show the largest SD, mainly due to representativeness errors as found by AR2018. The C2 and MERRA2 error SD are in the middle. The C2 random errors are similar to those of COSMIC (AR2018) as expected. Also shown in Figure 6 is the mean of the SD of the differences between C2 and each of the other four data sets (red profile). The SD of differences between two data sets is a common method of comparing the random errors of different data sets (Kuo et al., 2004). As shown in Figure 6, the 3CH estimates of the RO error SD are always less than the SD of the difference between RO and the other data sets.

3. Summary

Early results from the FORMOSAT-7/COSMIC-2 mission indicate that the stratospheric and tropospheric profiles of radio occultation bending angle and refractivity are meeting their high expectations. The mean and median SNR values are higher than any previous radio occultation mission, which enables deeper tropospheric penetration (50% within 200 m of Earth's surface) of the soundings. The higher SNR also enables better observation of the atmospheric boundary layer depth and detection of superrefraction on top of the atmospheric boundary layer.

Comparison of bending angle profiles from nearby C2 satellites shortly after launch demonstrates high precision of the data. Comparison of over 100,000 C2 vertical profiles of bending angles and refractivities from October 2019 with other independent data sets, including radiosondes, short-term operational forecasts, and the MERRA-2 reanalyses shows very small biases from about 2 to 40 km. Random error profiles of C2

refractivity are generally less in magnitude than radiosondes and the MERRA-2 reanalysis in the troposphere, but higher than the short-term forecasts. In the stratosphere, the C2 and radiosonde errors are comparable, and greater than those of the model data sets.

These results indicate that high-SNR C2 radio occultation soundings open up exciting new opportunities to study the challenging tropical atmosphere, will significantly benefit operational NWP forecasts and will provide valuable data of unprecedented quality that are freely available to the international scientific community.

Acknowledgments
FORMOSAT-7/COSMIC-2 is a partnership between the National Space Organization in Taiwan and NOAA, the U.S. Air Force, and the University Corporation for Atmospheric Research (UCAR) in the United States. The UCAR work is sponsored by NSF-NASA Grant 1522830, NOAA Contract 16CN0070, U.S. Air Force Contract 319C004 and NSPO-UCAR AIT-TECRO Agreement Implementing Arrangement 5. All data used in this paper are available from the UCAR COSMIC Data Analysis and Archive Center (www.cosmic.ucar.edu). Please contact the corresponding author for details on access.

References

Anthes, R.A. (2011). Exploring Earth's atmosphere with radio occultation: Contributions to weather, climate and space weather, *Atmos. Meas. Tech.*, *4*, 1077-1013, http://doi.org/10.5194/amt-4-1077-2011

Anthes, R., & Schreiner, W. (2019). Six new satellites watch the atmosphere over Earth's equator. *Eos*, *100*. https://doi.org/10.1029/2019EO131779

Anthes, R. A., & Rieckh, T. (2018). Estimating observation and model error variances using multiple data sets. *Atmospheric Measurement Techniques*, *11*(7), 4239–4260. https://doi.org/10.5194/amt-11-4239-2018

Ao, C. O. (2007). Effect of ducting on radio occultation measurements: An assessment based on high-resolution radiosonde soundings. *Radio Science*, *42*(2), RS2008. http://doi.org/10.1029/2006RS003485

Ao, C. O., Meehan, T. K., Hajj, G. A., Mannucci, A. J., & Beyerle, G. (2003). Lower troposphere refractivity bias in GPS occultation retrievals. *Journal of Geophysical Research*, *108*(D18), 4577. https://doi.org/10.1029/2002JD003216

Gelaro, R., McCarty, W., Suarez, M. J., Todling, R., Molod, A., Takacs, L., et al. (2017). The Modern-Era Retrospective Analysis for research and applications, Version 2 (MERRA-2). *Journal of Climate*, *30*(14), 5419–5454. http://doi.org/10.1175/JCLI-D-16-0758.1

Gilpin, S., Anthes, R., & Sokolovskiy, S. (2019). Sensitivity of forward-modeled bending angles to vertical interpolation of refractivity for radio occultation data assimilation. *Monthly Weather Review*, *147*(1), 269–289. https://doi.org/10.1175/MWR-D-18-0223.1

Gorbunov, M. E., & Kirchengast, G. (2018). Wave-optics uncertainty propagation and regression-based bias model in GNSS radio occultation bending angle retrievals. *Atmospheric Measurement Techniques*, *11*, 11–125. http://doi.org/10.5194/amt-11-11-2018

Gorbunov, M. E., Vorob'ev, V. V., & Lauritsen, K. B. (2015). Fluctuations of refractivity as a systematic error source in radio occultations. *Radio Science*, *50*(7), 656–669. http://doi.org/10.1002/2014RS005639

Heelis, R. A., Stoneback, R. A., Perdue, M. D., Depew, M. D., Morgan, W. A., Mankey, M. W., et al. (2017). Ion velocity measurements for the ionospheric connections explorer. *Space Science Reviews*, *212*(1-2), 615–629. https://doi.org/10.1007/s11214-017-0383-3

Ho, S.-P., Anthes, R.A., Ao, C.O., Healy, S., Horanyi, A., Hunt, D., et al. (2019). The COSMIC-FORMOSAT-3 radio occultation mission after 12 years: Accomplishments, remaining challenges, and potential impacts of COSMIC-2 (2019). *Bulletin of the American Meteorological Society*, *100*, online version: https://journals.ametsoc.org/doi/pdf/10.1175/BAMS-D-18-0290.1

Kuo, Y.-H., Wee, T.-K., Sokolovskiy, S., Rocken, C., Schreiner, W., Hunt, D., & Anthes, R. A. (2004). Inversion and error estimation of GPS radio occultation data. *Journal of the Meteorological Society of Japan*, *82*(1B), 507–531.

Li, Y., Kirchengast, G., Scherllin-Pirscher, B., Schwaerz, M., Nielsen, J. K., Ho, S.-P., & Yuan, Y.-B. (2019). A new algorithm for the retrieval of atmospheric profiles from GNSS radio occultation data in moist air and comparison to 1DVar retrievals. *Remote Sensing*, *11*, 2729. http://doi.org/10.3390/rs11232729

O'Carroll, A. G., Eyre, J. R., & Saunders, R. S. (2008). Three-way error analysis between AATSR, AMSR-E, and in situ sea surface temperature observations. *Journal of Atmospheric and Oceanic Technology*, *25*, 1197–1207. http://doi.org/doi:10.1175/2007JTECHO542.1

Rieckh, T., & Anthes, R. A. (2018). Evaluating two methods of estimating error variances using simulated data sets with known errors. *Atmospheric Measurement Techniques*, *11*, 4309–4325. https://doi.org/10.5194/amt-11-4309-2018

Sokolovskiy, S. (2003). Effect of superrefraction on inversions of radio occultation signals in the lower troposphere. *Radio Science*, *38*(3), 1058. http://doi.org/10.1029/2002RS002728

Sokolovskiy, S., Schreiner, W., Zeng, Z., Hunt, D., Lin, Y.-C., & Kuo, Y.-H. (2014). Observation, analysis, and modeling of deep radio occultation signals. Effect of tropospheric ducts and interfering signals. *Radio Science*, *49*, 954–970. http://doi.org/10.1002/2014RS005436

Sokolovskiy, S. V., Rocken, C., Lenschow, D. H., Kuo, Y. H., Anthes, R. A., Schreiner, W. S., & Hunt, D. C. (2007). Observing the moist troposphere with radio occultation signals from COSMIC. *Geophysical Research Letters*, *34*, L18802. https://doi.org/10.1029/2007GL030458

Syndergaard, S., (2018). Validation Report: Reprocessed Level 1B bending angle, Level 2A refractivity, Level 2A dry temperature CDR v1.0 products Version 1.2, 20 December 2018, SAF/ROM/DMI/REP/ATM/001, https://www.romsaf.org/product_documents/romsaf_vr_atm_rep.pdf

Sokolovskiy, S., Rocken, C., Schreiner, W., & Hunt, D. (2010). On the uncertainty of radio occultation inversions in the lower troposphere. *Journal of Geophysical Research*, *115*(D22). https://doi.org/10.1029/2010jd014058

Tien, J.Y., Okihiro, B. Bachman, Esterhuizen, S.X., Franklin, G.W., Meehan, T.K., Munson, T.N., et al. (2012). "Next generation scalable spaceborne GNSS science receiver," *Proceedings of the 2012 International Technical Meeting of The Institute of Navigation*, Newport Beach, CA, January 2012, 882-914.

Xie, F., Syndergaard, S., Kursinski, E. R., & Herman, B. M. (2006). An approach for retrieving marine boundary layer refractivity from GPS radio occultation data in the presence of super-refraction. *Journal of Atmospheric and Oceanic Technology*, *23*, 1629–1644. https://doi.org/10.1175/JTECH1996.1

Xie, F., Wu, D. L., Ao, C. O., Kursinski, E. R., Mannucci, A. J., & Syndergaard, S. (2010). Super-refraction effects on GPS radio occultation refractivity in marine boundary layers. *Geophysical Research Letters*, *37*, L11805. https://doi.org/10.1029/2010GL043299